Journal of Magnetic Resonance 291 (2018) 32–39

Contents lists available at ScienceDirect

Journal of Magnetic Resonance

journal homepage: www.elsevier.com/locate/jmr

^{1}H line width dependence on MAS speed in solid state NMR – Comparison of experiment and simulation

Ulrich Sternberg [a,b,*], Raiker Witter [c,d,e], Ilya Kuprov [f], Jonathan M. Lamley [g], Andres Oss [c,e], Józef R. Lewandowski [g], Ago Samoson [c,e]

[a] Karlsruhe Institute of Technology (KIT), Karlsruhe, Germany
[b] COSMOS GbR, Jena, Germany
[c] School of Information Technologies, Tallinn University of Technology, Tallinn, Estonia
[d] Institute of Nanotechnology, Karlsruhe Institute of Technology (KIT), Karlsruhe, Germany
[e] NMR Institute MTÜ, Tallinn, Estonia
[f] School of Chemistry, University of Southampton, UK
[g] Department of Chemistry, University of Warwick, Coventry, UK

ARTICLE INFO

Article history:
Received 30 November 2017
Revised 4 April 2018
Accepted 6 April 2018
Available online 7 April 2018

Keywords:
^{1}H solid-state NMR
High-speed MAS
MAS line widths
Spinach simulation
Fokker-Plank approach

ABSTRACT

Recent developments in magic angle spinning (MAS) technology permit spinning frequencies of ≥100 kHz. We examine the effect of such fast MAS rates upon nuclear magnetic resonance proton line widths in the multi-spin system of β-Asp-Ala crystal. We perform powder pattern simulations employing Fokker-Plank approach with periodic boundary conditions and ^{1}H-chemical shift tensors calculated using the bond polarization theory. The theoretical predictions mirror well the experimental results. Both approaches demonstrate that homogeneous broadening has a linear-quadratic dependency on the inverse of the MAS spinning frequency and that, at the faster end of the spinning frequencies, the residual spectral line broadening becomes dominated by chemical shift distributions and susceptibility effects even for crystalline systems.

1. Introduction

The superior sensitivity of ^{1}H detected experiments and the wealth of information on molecular structure and dynamics that they provide has always rendered observation of protons (^{1}Hs) as very important for the NMR spectroscopy. Without much of an exaggeration it is due to accessibility of ^{1}H NMR in liquid samples, where anisotropic interactions such as dipolar couplings and chemical shift anisotropy (CSA) are well-averaged by overall rotational diffusion, solution NMR has become an extremely powerful and widely applicable approach to study molecules at atomic resolution. In solids, however, high-resolution proton studies are hampered by the significant line-broadening effects due to the presence of strong homonuclear ^{1}H–^{1}H dipolar couplings. Despite this drawback, ^{1}H NMR in the solid state has found numerous applications, particularly in studies of small natural abundance organic molecules and their crystal polymorphs that are pharmaceutically relevant [1] but also, increasingly, for elucidation of structure and dynamics of biomolecules [2–7]. To combat the broadening effects of ^{1}H–^{1}H dipolar couplings and improve spectral resolution in ^{1}H observed spectra, studies usually employ either dilution of the dense networks of protons with deuterium atoms [8–10], combined rotation and multiple pulse spectroscopy (CRAMPS) techniques to decouple the homonuclear dipolar couplings [11–13] or combination of these two solutions [14]. The first of these approaches is most commonly used for proteins where incorporation of ^{2}H is achieved by biosynthetic methods [15]. For other systems where deuterated derivatives need to be synthesized chemically, this route is less common due to a more resource intensive nature of the approach. On the other hand, CRAMPS methods achieved a remarkable feat of efficient averaging of the ^{1}H–^{1}H dipolar couplings even under moderate spinning frequencies [16–25]. Thanks to this, investigations on uniformly protonated compounds have become increasingly popular in the recent years [18,21,26–34]. However, to obtain the optimum performance for CRAMPS techniques effects of pulse imperfections, specifics of hardware, details of irradiation schemes, intricacies of windowed acquisition and related artifacts, etc. have to be considered. Because of that homonuclear decoupling sequences typically require optimization of experimental parameters [16,35].

* Corresponding author at: Karlsruhe Institute of Technology (KIT), Karlsruhe, Germany.
E-mail address: ulrich.sternberg@partner.kit.edu (U. Sternberg).

https://doi.org/10.1016/j.jmr.2018.04.003
1090-7807/

Consequently, routine implementations of CRAMPS methods require a considerable level of technical expertise from operators. In addition, because application of homonuclear decoupling scales down the chemical shifts and the theoretical scaling factors often differ from the experimental ones, proton chemical shifts need to be corrected by comparing the decoupled spectra to spectra where the dipolar coupling averaging is accomplished using only MAS [21,29,36]. Finally, the losses of magnetization during application of CRAMPS methods mean that the full potential of ^{1}H detected experiments is not yet fully exploited. In spite of these challenges the numerous applications enabled by CRAMPS are a testament to desirability and wide scope of applications of ^{1}H spectroscopy.

The promise to achieve similar or better resolution as the one afforded by CRAMPS methods but without the associated challenges renders ^{1}H spectroscopy enabled by fast spinning highly desirable [37]. To guide such experiments and to understand their intrinsic limitations, in this contribution we estimate the extent to which the powder lines can be narrowed by MAS.

In the absence of extensive dynamics and special cases such as e.g. in the presence of paramagnetic centers, the majority of solid state ^{1}H line widths is due to two different effects: (i) homogenous broadening primarily due to strong dipolar couplings and to a lesser extent ^{1}H–^{1}H J-couplings (in the case of the dipeptide with isotropic values of up to 20 Hz) and (ii) inhomogenous broadening due to B_0 field inhomogeneities, magnetic field variation in powdered samples caused by susceptibility distribution (anisotropic bulk magnetic susceptibility) due to variation of particle/crystal shapes and chemical shift dispersion caused by disorder/defects in the sample. In proteins where slow molecular motions play a much more prominent role than in small molecules, homogenous broadening from relaxation can also be a significant factor [3,4]. Inhomogeneous broadening scales linearly with magnetic field strength and is re-focused by 180° pulses [38] but stays constant when measured in ppm. Notably, this effect survives averaging by MAS (and CRAMPS as well) and will lead to residual broadening even under infinitely fast MAS. One of the goals of this investigation is to provide estimation for this source of broadening in a small molecule polycrystalline sample in the regime where the homogenous broadening becomes increasingly small.

Homogeneous line broadening can be separated from inhomogeneous broadening by measuring the coherence lifetimes, T_2', during a spin echo experiment [39,40]. As discussed by Levitt *et al.* in the context of spin pairs the MAS line width should be proportional to $1/\omega_{MAS}$ or $1/(\omega_{MAS})^2$ depending on the chemical shifts (CS) and the CS tensors of the coupled nuclei [41]. Brunner *et al.* considered the dependence of the line width on spinning frequency in analysis that included the geometry of the network of the coupling nuclei [42]. Since the Hamiltonian of a dipolar network of like spins such as protons does not, in general, commute with itself at different times, the analytical treatment of the homogeneous broadening effect is mostly limited to simple manageable cases. Here we were able to perform rigorous simulations of homogenous proton broadening on a multiple spin system consisting of a much more realistic number of spins compared to studies found in the literature. Our simulations are based on the Fokker-Plank equations applied to a crystal lattice with periodic boundary conditions and calculated ^{1}H chemical shift anisotropy [43]. A direct comparison with experimental results allows the extraction of simple rules for the line narrowing effect due to fast MAS. Our simulations avoid most limitations that hampered numerical simulations in the past [44]. These investigations aid in guiding the relatively straightforward and time-efficient "fast MAS only" method that is appropriate for the characterization of small organic molecules at natural abundance (i.e. without any isotopic enrichment) in the solid state.

2. Experimental

NMR experiments were performed on a 850 MHz Bruker Avance III spectrometer using a triple resonance 0.81 mm probe (Fig. 1) developed in the Samoson laboratory. The rotor size was carefully optimized for the sensitivity. In the final design sample with volume of ~700–800 nL could spin at ~100 kHz. Powdered natural abundance β-L-Asp-L-Ala dipeptide was purchased from Bachem and packed, without further re-crystallization, into a 0.81 mm rotor. The adjustment of the magic angle was carried out at 80 kHz spinning speed via line width observation and minimization for ^{1}H spectra. 1D ^{1}H spectra of the dipeptide were obtained over a range of spinning frequencies ($\omega_r/2\pi$) between 15 and 100 kHz (±50 Hz). A spin-echo experiment was employed to improve the spectral baseline, with a total echo length (2τ) of 24 rotor periods [32]. Spin-echo experiments were also performed at different spinning frequencies in the range between 15 and 100 kHz to measure, for each proton in the dipeptide, the transverse dephasing time in the absence of inhomogeneous broadening (T_2') [40]. These experiments were repeated to account for the effects of sample temperature on the line widths. A Bruker BCU-X cooling unit was used with the target temperature set to −80 °C and the input nitrogen gas pressure set to 0.2 bar for relevant spinning frequencies (leading to different internal sample temperatures at different spinning frequencies). While the exact sample temperature was not known, application of cooling compensated for the frictional sample temperature rise and no difference in linewidth was observed consistent with a lack of extensive molecular motions in the molecule. In the subsequent experiments on proteins with internal chemical shift reference and water chemical shift as the indicator of sample temperature, we learned that in a 0.81 mm probe the frictional heating varies between 5 and 10 °C at ~90 kHz and reaches over 20 °C at 100 kHz (resulting in the overall sample temperature of ~45–50 °C if no cooling is applied).

Spectral line widths were obtained by fitting the ^{1}H spectra with ACD/NMR Processor. Each line width presented corresponds to the mean value of five independent fits (for which the peak

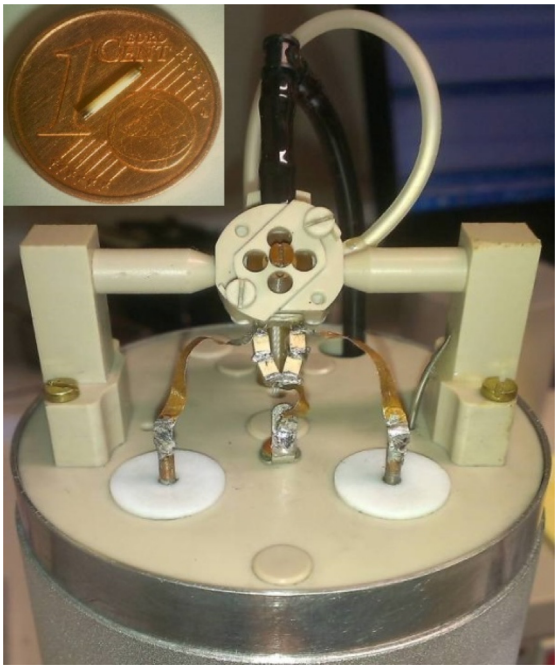

Fig. 1. Triple resonance magic angle spinning NMR probe with 0.81 mm rotor module capable of spinning to 100 kHz.

height, width, position and Lorentzian/Gaussian fraction were optimized) of the same spectrum, with varying starting fitting conditions. The standard deviations of the resulting width calculations were interpreted as the experimental errors. It should be noted that at lower spinning frequencies, these uncertainties were mostly larger due to the unresolved nature of the spectra, which meant that the same overall spectrum could be recreated from a range of close to equivalent solutions. T_2' values were estimated by fitting in Origin 8.5 [45] the signal intensity decay curves from spin echo experiments. For each curve, the points were obtained by taking the intensities of the relevant deconvoluted resonances of the spectra. The spin-echo line widths - homogeneous linewidths - were calculated as $1/(\pi T_2')$, with errors propagated by fit variations from related T_2' calculations.

3. Simulations

3.1. Structure modeling and NMR calculations

The crystal structure of a β-L-Asp-L-Ala dipeptide [46] was obtained from the Cambridge Crystallographic Data Centre [47] (CSD refcode FUMTAI). The original CIF-file (space group P212121) was transformed into a COSMOS [48] coordinate coo-file. The symmetry operations of the space group P212121 were executed on the non equivalent sites using COSMOS to generate all atoms within the unit cell. The cell contained 4 zwitterions with 4 equivalent sets of 12 protons (see Fig. 1 in Supplementary Materials) giving finally a spin system with 48 protons. By applying periodic boundary conditions on this spin matrix ($3 \times 3 \times 3 \times 48 = 1296$ spins) we obtained one of the most realistic model of ^{1}H network used for simulations to date (also see state of the art by Hodgkinson *et al.* [49,50]). For protons of the CH_3 and NH_3 groups which experimentally provide only single resonances, we distinguished all 8 different signals by the simulations (see Table 1 in Supplementary Materials). All dipolar couplings and chemical shift tensors were considered. ^{1}H shielding tensors have to be taken into account because their orientation dependences in respect to dipolar interactions are not negligible (e.g. level crossing during MAS) [51]. All nuclear shielding tensors were calculated using the bond polarization theory [52–54] (BPT). Due to the zwitterionic character of the crystal molecules within the unit cell, wide-ranging polarization effects had to be considered by taking periodic boundary conditions into account. By these means atomic charges and shielding tensors were calculated and included in the spin matrix (see Supplementary Materials for details).

BPT calculations are well suited for shielding tensor predictions (see Supplementary Materials Figs. 2a and 2b: $R > 0.992$ and error RMDS < 1.6 ppm). However, the accuracy of the isotropic values was further improved by shifting the tensor traces to the mean experimental values. The proton sites of the unit cell including the CS tensors were saved to a COSMOS coordinate file as an input for the simulations with Spinach.

3.2. Spectra simulations

The MAS powder pattern simulations were performed using the Spinach [55] simulation package written as a set of MATLAB [56] functions. The routines for the Fokker-Plank calculations [57] of the Spinach library were executed from a program controlling the input of the COSMOS coordinate files, data handling, powder averaging which also allowed to set the parameters of the NMR experiment. The simulation routine was complemented by a script for exporting graphics and spectra. A special routine was included that allowed to sample separate FIDs of all 48 proton sites to analyze all T_2' decay times. The unbiased 48 complex FIDs were stored in a file for further analysis.

Spinach simulations were carried out as batch processes on a high-performance computing cluster of Tallinn University of Technology. The powder averaging was simultaneously performed with parallelized algorithms on 12 processors. The simulations were performed using "spinach_1.4.2313" requiring at least MATLAB version R2013b (64-bit). Related Spinach version facilitates the usage of crystallographic periodic boundary conditions. The atoms of a unit cell must be provided as an input and then the periodic continuation is generated automatically. A single simulation with such unit cell consumed between 6 (15 kHz MAS) and 10 days (120 kHz MAS) of total computating time.

Spinach read directly Cartesian coordinates and calculated all dipolar interactions of the spin system. The CS tensors were imported from COSMOS coordinate file. Periodic boundary conditions were applied to the unit cell with a dimension of a = 4.845 Å which has been only slightly larger than the used dipolar cut off radius of 4 Å. Since proton interactions between connected unit cells were considered, realistic NMR signals can be expected.

Under experimental conditions (~300 K) the NH_3 and CH_3 groups undergo rotational jumps or diffusion which partially averages out their dipolar interactions on the NMR time scale. As an approximation for the influence of this effect, we set all dipolar coupling values of the protons within these groups to zero.

Spectra were obtained by fast Fourier transformation of the original simulated FIDs. FIDs were preprocessed using zero filling and gentle exponential apodization. The simulated FIDs did not decay to zero (see Fig. 3 is Supporting Materials). We increased the exponent for the apodization until the Fourier transform artifacts from the step contribution just started to disappear. Despite the fact that the apodization added 82 Hz to the line widths the simulated spectra display sharper lines than the experimental ones (see Fig. 2) because the applied line broadening is still smaller than inhomogeneous line width in the sample used in the experiments (see Table 2). Resulting spectra could be analyzed by fitting resonances to Lorentzian line-shapes (see Figs. 5a and 5b in Supplementary Materials) but spectra cannot be expected to provide the quantitative identity of the influence of MAS on the residual line widths which are dominated at high speed by susceptibility and disorder effects. Only the homogeneous part of the line widths can be compared and interpreted. This part is related to T_2' decay time measured during spin echo experiments. We decided to determine T_2' directly from simulated FIDs. In a model-free-approach of the form of decay only absolute values of the 48 complex FIDs were used. The T_2' timings were obtained by searching for the time interval where the intensity dropped to $1/e$ of the values with respect to the zero-time-point. This procedure can be performed for all kinds of decaying functions disregarding the special functional forms. From all 48 individual positions, similar protons were averaged to obtain the 8 detectable mean T_2' values (for the complete setup of the simulations see Supplementary Materials).

4. Results and discussion

To observe the effect of increasing MAS on averaging of proton line widths, we measured 1D ^{1}H spectra on the dipeptide β-Asp-Ala at spinning frequencies from 15 to 100 kHz at 850 ^{1}H Larmor frequency, without homonuclear decoupling but with ^{13}C decoupling (Figs. 2a and 2b).

At the lowest considered MAS spinning frequency of 15 kHz, the simulation indicates (Fig. 4 in Supplementary Materials) that the rotational sidebands start to separate from the central lines. Due to the dominating dipolar broadening individual lines cannot be easily identified. Predictably, more peaks become resolved as ω_r

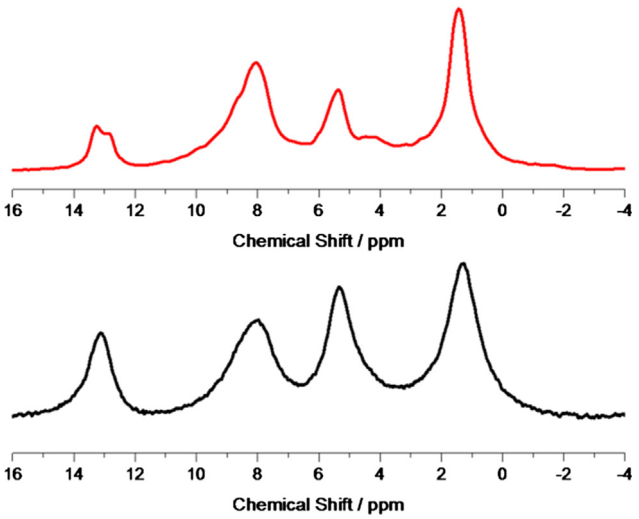

Fig. 2a. Simulated (top panel, red) and experimental (bottom panel, black) 1D ^{1}H NMR spectra of β-Asp-Ala at 15 kHz MAS frequency. (For interpretation of the references to color in this figure legend, the reader is referred to the web version of this article.)

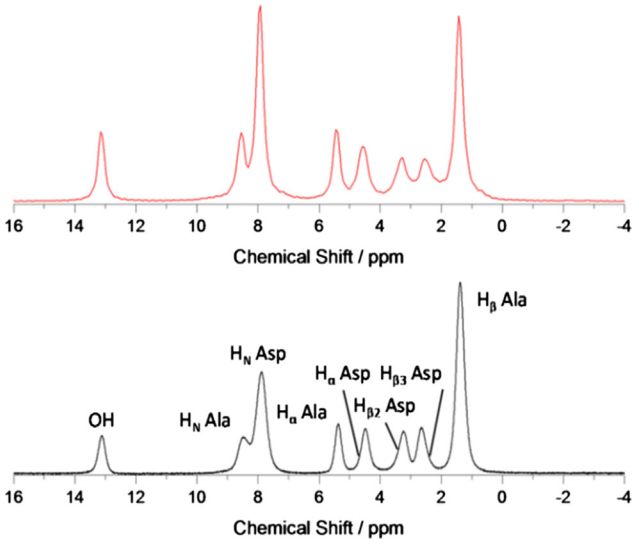

Fig. 2b. Simulated (top panel, red) and experimental (bottom panel, black) 1D ^{1}H solid-state NMR spectra of β-Asp-Ala at 100 kHz MAS frequency. (For interpretation of the references to color in this figure legend, the reader is referred to the web version of this article.)

is increased; with the two Asp CH_2 proton resonances becoming resolved at around 65 kHz (see Supplementary Materials Fig. 6) where corresponding resonances have line widths of 418 ± 5 and 351 ± 1 Hz (0.49 ppm and 0.41 ppm, $H_{\beta 2}$ and $H_{\beta 3}$ Asp respectively). The distance between the two protons of CH_2 groups give rise to a dipolar coupling of 64.3 kHz (see Table 1) and obviously we have to spin at least with a similar minimum frequency to separate the lines of the sites. At 850 MHz ^{1}H Larmor frequency and 100 kHz spinning the line width of the CH_2 protons becomes 0.34 ppm ($H_{\beta 2}$: 292 ± 1 Hz) and 0.32 ppm ($H_{\beta 3}$: 274 ± 2 Hz, see Table 2).

These are comparable to the 0.36 ppm and 0.34 ppm improved line widths that had been achieved using eDUMBO-PLUS-1 homonuclear decoupling scheme at a similar field strength (800 MHz) [18]. Thus line narrowing at 100 kHz spinning is comparable to the state of the art high power homonuclear decoupling at lower spinning frequencies. One of the obvious benefits of the approach based on fast magic spinning is its simplicity. At a given temperature, the extent of obtained line-narrowing only depends on the precision of the magic angle setting and quality of shimming, both of which would be required for any other type of experiment setup, e.g. CRAMPS. Another major advantage is that intensities of chemical shift resonances which are reflecting certain molecular environments are directly proportional to a number of related proton spins: ^{1}H concentrations can be directly extracted from such spectra without any special manipulation or rescaling.

The contributions to the proton line widths can be grouped into two categories: homogeneous broadening and inhomogeneous boradening. Homogenous broadening is dominated by the incomplete averaging of homonuclear dipolar couplings, which can be reduced by MAS, with contribution from transverse relaxation. Inhomogeneous broadening due to field alternations and disorder within the sample cannot be eliminated by spinning (or CRAMPS) without removing chemical shift information. As such it is useful to separate the two broadening components and compare experiments with realistic calculations. In order to remove the inhomogeneous part, we measured the transverse dephasing time of protons during the spin-echo experiments, T_2' [40], as a function of spinning frequency, in the 30–100 kHz range. For 100 kHz spinning the values are compiled in Table 1 (and Fig. 7 of Supplementary Materials) which shows the MAS frequency dependence of the total and spin-echo line widths (equal to $1/(\pi T_2')$) of the protons in β-Asp-Ala. It has been found in numerous other studies that line widths decrease with increasing ω_r since the dipolar couplings are averaged out more effectively. The offset between the two sets of data for each proton (total broadening and homogeneous broadening) represent the inhomogeneous contribution of the line width, which is not refocused in a T_2 measurement. Although the inhomogeneous contribution is approximately constant with varying ω_r, [38] the offset is site-specific. The amount of such inhomogeneous broadening in this particular polycrystalline β-Asp-Ala sample is typically > 125 Hz (> 0.15 ppm). The absolute spin-echo line widths should, however, be considered with some degree of caution, as systematic errors can arise in cases where a single exponentials fit the T_2 data rather poorly (we recognized such deviations in our simulation results) [38].

The line width dependency on ω_r has been investigated previously. For instance, Zorin *et al.* [44] used a semi-analytical approach of dipolar interacting spin systems to show a $1/\omega_r$ dependency of line width. This analysis disregards the influences of chemical shift tensors. Brunner *et al.* [42] assumed that the ^{1}H CS tensors should be axially symmetric (skew +1 or −1) which doesn't reflect the results of our COSMOS BPT-calculations (see evaluation results in Table 2 of Supplementary Materials). Since our simulations of spectra included realistic ^{1}H CS tensor values for of each site their relative influence can be understood in detail. First of all, it is clear that the influence of rotational resonances [41] even at lowest spinning frequency of 15 kHz can be excluded: such conditions may occur if the differences of isotropic shifts of two sites are equal to a multiple (n) of the rotational frequency ($\Delta\omega^{iso} \approx n\omega_r$). In our experiments, the largest possible CS difference of 11.7 ppm yields $\Delta\omega^{iso}/2\pi$ of 10.5 kHz.

When discussing the ω_r dependency of the line width three cases have to be distinguished: (i) case of negligible small CS difference ($\Delta\omega^{iso} \approx 0$), (ii) case where the chemical shift difference is on the same order of magnitude as the dipolar coupling ($\Delta\omega^{iso} \approx \omega^{dip}$) and (iii) case where the chemical shift difference exceeds the dipolar coupling ($\Delta\omega^{iso} \gg \omega^{dip}$). In the limit of case (iii) the flip-flop term of the interaction Hamiltonian can be neglected [41] and the Hamiltonian has then a similar form as a hetero-nuclear spin interaction. Such an operator is self-commuting and behaves like an

Table 1
Observed ^{1}H chemical shift differences and calculated dipolar couplings to the nearest neighbor proton sites. The shift difference in frequency units is displayed in the last column. The ^{1}H dipolar couplings within the CH_3 and NH_3 groups are not displayed.

Proton Site	Chemical Shift, ppm	Nearest Neighbor	DD Coupling Const. to Nearest Neighbor, kHz	$\Delta\omega^{iso}/2\pi$, kHz
H (OH)	13.1	H_α Asp	15.60	7.22
H_N Ala	8.5	$H_{\beta 2}$ Asp	24.05	4.45
H_N Asp[a]	7.9	H_{NH} Asp[a]	14.36, 4.58, 12.71	4.37
H_α Asp	4.5	H(OH)	15.60	7.22
$H_{\beta 2}$ Asp	3.2	H(OH)	64.32	0.50
$H_{\beta 3}$ Asp	2.6	$H_{\beta 3}$ Asp	64.32	0.50
H_α Ala	5.4	$H_{\beta 2}$ Asp	17.36, 10.198, 17.37	3.56
H_β Ala[a]	1.4	H_β Ala[a],H_N Ala	17.37, 10.18, 17.37	3.56
		H_β Ala[a],H_α Ala		

[a] The chemical shifts are mean values of 3 protons of a CH_3 or NH_3 group resp.

Table 2
Total, homogeneous and inhomogeneous limit ^{1}H line widths of β-Asp-Ala, measured at 100 kHz MAS spinning and 850 MHz ^{1}H Larmor frequency. Inhomogeneous limit values indicate the minimum line width that may be measured on this sample at an infinite spinning frequency which reflects the contributions from inhomogeneous broadening, ^{1}H–^{1}H J-couplings (here up to 20 Hz) and relaxation.

Peak	H(OH)	H_N Ala	H_N Asp	H_α Ala	H_α Asp	$H_{\beta 2}$ Asp	$H_{\beta 3}$ Asp	H_β Ala
Line width/Hz (ppm)	229 ± 1 (0.27)	339 ± 5 (0.40)	325 ± 2 (0.38)	211 ± 0.5 (0.25)	295 ± 1 (0.30)	292 ± 0.5 (0.34)	274 ± 2 (0.32)	269 ± 0.5 (0.32)
Spin-echo line width/Hz (ppm)	78 ± 9 (0.09)	146 ± 38 (0.17)	174 ± 15 (0.20)	71 ± 10 (0.08)	138 ± 25 (0.16)	290 ± 130 (0.34)	240 ± 120 (0.28)	136 ± 6 (0.16)
Inhomogenous limit line width/Hz (ppm)	147 ± 23 (0.17)	170 ± 10 (0.20)	164 ± 16 (0.19)	135 ± 5 (0.16)	84 ± 8 (0.10)	142 ± 29 (0.17)	163 ± 12 (0.19)	166 ± 12 (0.20)

inhomogeneous contribution under MAS, i.e. produces sharp splitting in the spectrum but cannot be re-focused with a 180° spin-echo. In our simulations, we frequently encountered the intermediate scenario (ii) where $\Delta\omega^{iso}$ and ω^{dip} are in the same order of magnitude. In this case, we should observe a decrease of the line width with the inverse of the MAS rate squared [41]: $1/(\omega_r)^2$. Since the Hamiltonian for this case does not commute with itself at different times, the interaction is called homogeneous and is not re-focused in spin-echo experiments. If the coupling nuclei have negligible CS differences (i) we have the case of so-called "$n \approx 0$ rotational resonances" [41]. Since in our simulations also the CS anisotropy is present this effect does occur if the principal axes of the CS tensors of the coupling nuclei do not coincide. This effect has essentially the same behavior as a case (ii) and leads to a homogeneous broadening of the MAS line with a narrowing related to $1/(\omega_r)^2$. These cases that are discussed above are strictly valid only for isolated spin pairs but the theory [41] provides some guidelines to tackle the case of an interacting multi-spin system.

For the simulated spectra, we needed to introduce apodization which introduced artificial broadening mostly reflecting the inhomogeneous contributions but not the influence of MAS. Therefore, only the homogeneous part of the line widths is considered under thorough theoretical investigations involving magnetization decay time T_2 in spin echo experiments. A direct determination of T_2 from the calculated FID was obtained avoiding any data processing. The collected theoretical data of T_2 as a function of MAS frequency

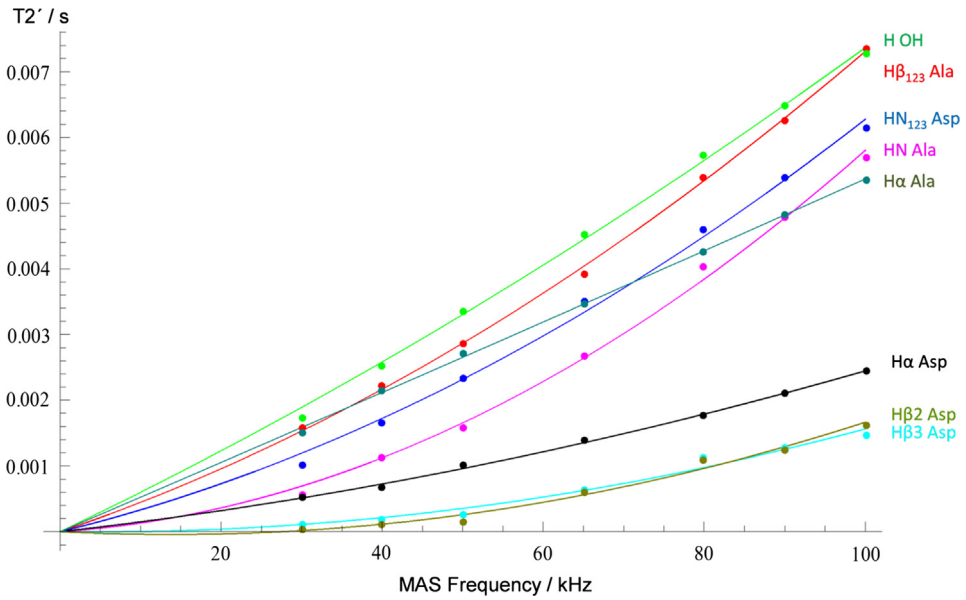

Fig. 3. Simulated T_2' times at spinning frequencies from 30 to 100 kHz. The lines are obtained by fitting the data to a linear-quadratic dependence. Values of *a* and *b* parameters are given in Table 3.

$\nu_r = \omega_r/2\pi$, can be seen in Fig. 3. Strikingly, all simulated T_2'-curves follow a linear-quadratic model of the following form:

$$T_2' = a\nu_{MAS} + b\nu_{MAS}^2$$

It is not possible to derive the linear-quadratic trend of T_2' on the MAS frequency directly from the line widths dependence on $1/\omega_r$ and $1/(\omega_r)^2$ but we represent two limiting cases - T_2' proportional to ν_{MAS} if the $1/(\omega_r)^2$ term is vanishing and T_2' proportional to $(\nu_{MAS})^2$ if the $1/\omega_r$ term is zero. The linear-quadratic dependence of T_2' on the MAS frequency should, therefore, be regarded as the first two-term of a power series of T_2' with respect to ν_{MAS}. The two limiting cases can be readily identified in our simulations (see Fig. 3 and Table 3): T_2' of H_α Ala has a nearly linear dependence on ν_{MAS} and for $H_{\beta2}$ and $H_{\beta3}$ of Asp the linear term is approximately zero and only the quadratic term remains. For H_α Ala echo decay times are dominated by a $1/\omega_r$ dependence, which is reflected by the parameters a and b (see Table 3): H_α Asp has a much smaller quadratic term compared to the other proton sites. $H_{\beta2}$ Asp and $H_{\beta3}$ Asp have the lowest linear contribution and follow dependency closer to $1/(\omega_r)^2$ in accordance with the findings of Levitt *et al.* [41]. The obvious differences between the proton sites display some regular patterns when looking at the nearest neighbors (see Table 1). The CH_2 protons have the largest dipolar interaction (64.32 kHz) and the smallest CS difference (0.5 kHz) such that they have the smallest linear term a. The proton of the OH-site has a small quadratic term b and a large linear term a corresponding to CS difference to H_α Asp with 7.22 kHz and a dipolar coupling of only 15.6 kHz. But these rules are to be taken with care since they involve only isolated spin pairs. Until now there is no theory for the parameters a and b of the linear-quadratic dependency of T_2' on ν_{MAS} but some trends can be observed how a and b depend on the NMR parameters $\Delta\omega^{is}$ and ω^{dip}. For NMR experimentalists, it is encouraging that proton lines with a small difference in CS but a large dipolar interaction are narrowed in a quadratic manner with the MAS frequency.

Having considered extended Spinach simulations the question arises whether calculated trends are also consistent with experiments. Fig. 4 shows plots correlating the theoretical and experi-

Table 3
Best fit parameters for the fit of the T_2' times to a linear-quadratic model of the form: $T_2' = a\nu_{MAS} + b\nu_{MAS}^2$ (ν_{MAS} in kHz, see Fig. 3).

Proton resonance	Parameter a × 10^{-5}	Parameter b × 10^{-7}
H_β Ala (CH_3)	4.158	3.151
H(OH)	5.848	1.519
H_N Asp (NH_3)	2.997	3.279
H_N Ala	0.814	4.988
H_α Asp	1.395	1.052
$H_{\beta2}$ Asp	(0.0)-0.147[a]	1.710
$H_{\beta3}$ Asp	(0.0)-0.633[a]	2.298
H_α Ala	5.243	0.126

[a] Within the error limits these values should be zero.

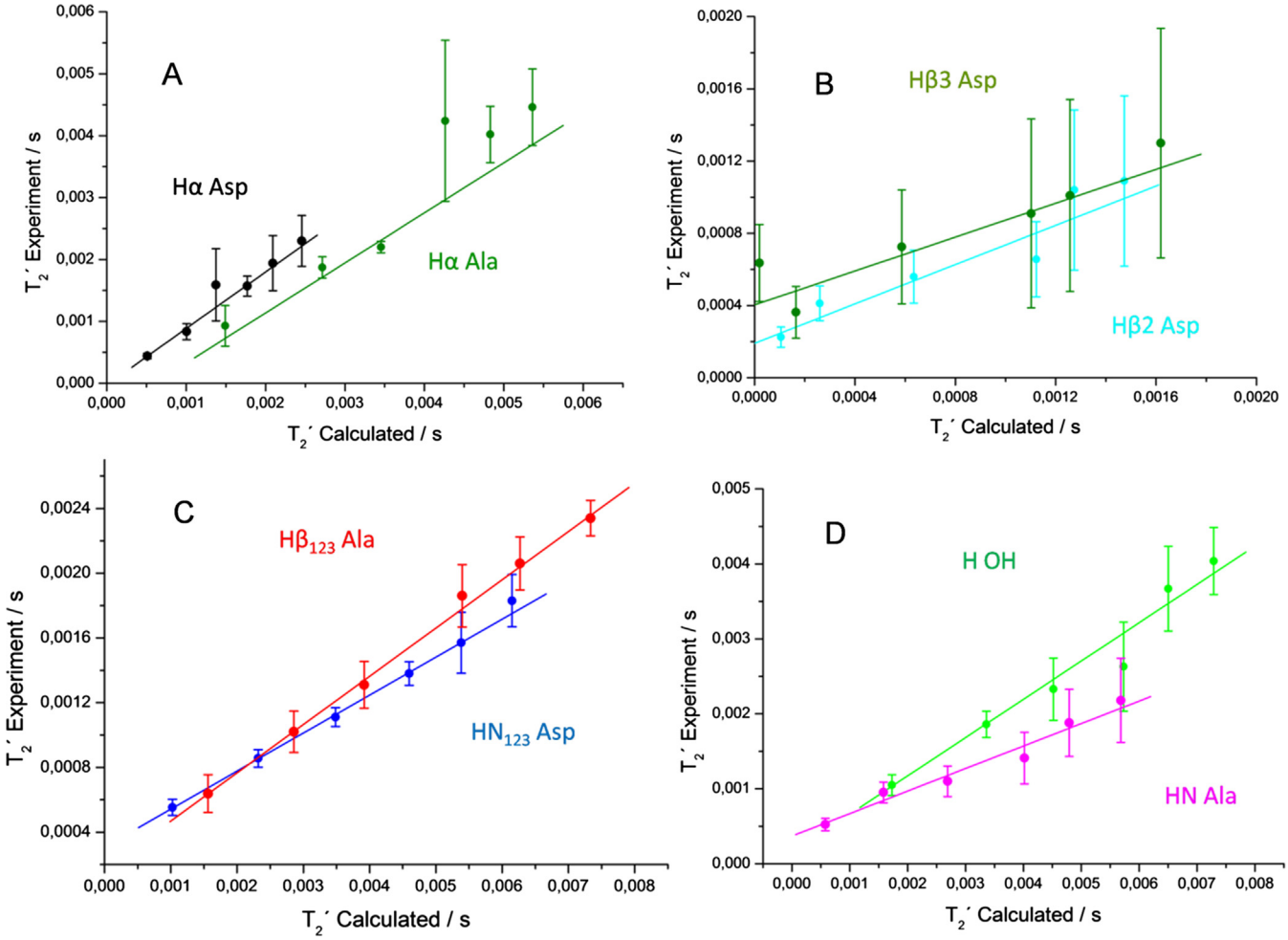

Fig. 4. Correlation plots for the simulated and experimental ^1H T_2 times in β-L-Asp-L-Ala. The color code is the same as in Fig. 3. The lines represent linear fits of the correlation data between calculated and experimental values. (For interpretation of the references to colour in this figure legend, the reader is referred to the web version of this article.)

mental T_2 times, which exhibit linear correlation within the experimental error bounds. Ideally, the slope of the linear correlations should be close to 1.0 and the lines crossing with the ordinate at zero point. However, such behavior is only met for H_α Ala and H_α Asp (panel A in Fig. 3 and Table 5 in Supplementary Materials). All other proton sites theoretically provide a slope smaller than 1.0 which indicates a lower simulated homogeneous line width than observed in the experiment. The main reason for that might be the neglecting of homonuclear scalar J couplings (up to 20 Hz) and disregarding of relaxation due to molecular motion. Rotation or fast jumps of the CH_3 and NH_3 groups not only influence corresponding protons of the groups but also scale down the dipolar interactions to protons in the neighborhood. The dipolar interactions within those groups were set to zero but this treatment might need an improvement in future simulations. In particular, for the NH_3 group, the considered approximation yields a slope of only 0.24. It is known that NH_3 protons are forming hydrogen bonds to carbonyl oxygen atoms (see Fig. 1 in Supplementary Materials) that will slow down the motion of this group, with the result of a larger line width than in the case of CH_3 protons which are much less affected by hydrogen bonds.

We could use the determined trends of ^{1}H line widths as a function of the spinning frequency to evaluate benefits of developing even faster spinning probes than currently available. The broadest ^{1}H resonances in the considered here dipeptide and probably also in most other organic compounds originate from the CH_2 protons with a large dipolar interaction of more than 60 kHz. Based on the determined in our work trends to reduce homogeneous line widths by a factor of 2 one has to raise the spinning by a factor of $\sqrt{2}$. Thus even for CH_2 protons in β-L-Asp-L-Ala an increase of the spinning rate from 100 to 141 kHz would result in a homogenous line broadening of 0.2 ppm (170 Hz) which becomes on the order of inhomogeneous line broadening of powdered polycrystalline samples. Considering the minimum inhomogeneous contributions reported in the literature for single crystals of glycine, the total line width can be around 120 Hz [58] for CH_2, i.e. a further increase in MAS spinning speed up to 200 kHz for strongly coupled protons and beyond for other ^{1}H sites might still considerably improve the resolution.

5. Conclusions

The Spinach Fokker-Plank approach using PBC with COSMOS/BPT chemical shift tensor values and crystal coordinates of β-L-Asp-L-Ala dipeptide has been successfully applied for MAS spin-echo simulations from 15 to 100 kHz spinning frequencies. Subtle details of spectra were faithfully reproduced by simulation, validating our computational approach to a complicated many-spin and time-dependent problem. The ^{1}H homogeneous line broadening had been extracted and provided as simplest description a linear-quadratic dependency of T_2 on ν_{MAS}, i.e. the two terms represent the limiting cases with vanishing $1/\omega_r$-term or vanishing $1/(\omega_r)^2$-term. At spinning frequencies on the order of 100 kHz, inhomogeneous broadening starts becoming a dominant or at least non-negligible factor even in crystalline systems but the coherence lifetimes are increasing dramatically, in fact, faster than previously thought. The quadratic improvement of ^{1}H coherence lifetimes as a function of spinning frequency will be particularly beneficial for applications involving scalar couplings for polarization transfer, which have a theoretical 100% efficiency. The simple linear-quadratic dependence of T_2 on the MAS frequency allows an easy estimate of the ^{1}H line widths at higher spinning speed from preliminary experiments.

We show that at 100 kHz MAS frequencies and 850 MHz ^{1}H Larmor frequency, high-quality proton spectra can be obtained on powdered samples with ^{1}H line widths in the same order as those achievable with state of the art homonuclear decoupling schemes under optimal conditions. This work and other impressive examples reported recently in the literature suggest that the approach relying on ^{1}H detected spectroscopy at $\geq$100 kHz spinning should be widely applicable both to small as well as large molecules especially for material, medical and biological applications.

Acknowledgments

We are grateful to Prof. Steven Brown for providing the β-Asp-Ala sample. JML acknowledges support from the EPSRC. The UK 850 MHz solid-state NMR Facility used in this research was funded by EPSRC and BBSRC, as well as the University of Warwick, including part funding through Birmingham Science City Advanced Materials Projects 1 and 2 supported by Advantage West Midlands (AWM) and the European Regional Development Fund (ERDF). JRL acknowledges funding from Royal Society Grant RG130022, EPSRC Grant EP/L025906/1, ERC Starting Grant 639907, BBSRC Grant BB/L022761/1 and Gates Foundation OPP1160394. RW is gratefully acknowledging Tallinn University of Technology and Karlsruhe Institute of Technology. Funding from ESF and ETAG for project PUT126 as well as PUT1534 is acknowledged.

Appendix A. Supplementary material

Supplementary data associated with this article can be found, in the online version, at https://doi.org/10.1016/j.jmr.2018.04.003. Raw ^{1}H spectra are available on Mendeley Data at https://doi.org/10.17632/rrc9pzc4wk.1.

References

[1] S.P. Brown, Applications of high-resolution H-1 solid-state NMR, Solid State Nucl. Mag. 41 (2012) 1–27.
[2] L.B. Andreas, K. Jaudzems, J. Stanek, D. Lalli, A. Bertarello, T. Le Marchand, D.C. D. Paepe, S. Kotelovica, I. Akopjana, B. Knott, S. Wegner, F. Engelke, A. Lesage, L. Emsley, K. Tars, T. Herrmann, G. Pintacuda, Structure of fully protonated proteins by proton-detected magic-angle spinning NMR, P. Natl. Acad. Sci. USA 113 (2016) 9187–9192.
[3] J.M. Lamley, C. Oster, R.A. Stevens, J.R. Lewandowski, Intermolecular interactions and protein dynamics by solid-state NMR spectroscopy, Angew. Chem. Int. Ed. 54 (2015) 15374–15378.
[4] J.M. Lamley, D. Iuga, C. Oster, H.J. Sass, M. Rogowski, A. Oss, J. Past, A. Reinhold, S. Grzesiek, A. Samoson, J.R. Lewandowski, Solid-state NMR of a protein in a precipitated complex with a full-length antibody, J. Am. Chem. Soc. 136 (2014) 16800–16806.
[5] E. Barbet-Massin, C.T. Huang, V. Daebel, S.T.D. Hsu, B. Reif, Site-specific solid-state NMR studies of "Trigger Factor" in complex with the large ribosomal subunit 50S, Angew. Chem. Int. Ed. 54 (2015) 4367–4369.
[6] J.P. Demers, V. Chevelkov, A. Lange, Progress in correlation spectroscopy at ultra-fast magic-angle spinning: basic building blocks and complex experiments for the study of protein structure and dynamics, Solid State Nucl. Mag. 40 (2011) 101–113.
[7] C. Oster, S. Kosol, C. Hartlmuller, J.M. Lamley, D. Iuga, A. Oss, M.L. Org, K. Vanatalu, A. Samoson, T. Madl, J.R. Lewandowski, Characterization of protein-protein interfaces in large complexes by solid-state NMR solvent paramagnetic relaxation enhancements, J. Am. Chem. Soc. 139 (2017) 12165–12174.
[8] A.E. Mcdermott, F.J. Creuzet, A.C. Kolbert, R.G. Griffin, High-resolution magic-angle-spinning nmr-spectra of protons in deuterated solids, J. Magn. Reson. 98 (1992) 408–413.
[9] L. Zheng, K.W. Fishbein, R.G. Griffin, J. Herzfeld, 2-Dimensional solid-state H-1-Nmr and proton-exchange, J. Am. Chem. Soc. 115 (1993) 6254–6261.
[10] B. Reif, C.P. Jaroniec, C.M. Rienstra, M. Hohwy, R.G. Griffin, 1H–1H MAS correlation spectroscopy and distance measurements in a deuterated peptide, J. Magn. Reson. 151 (2001) 320–327.
[11] B.C. Gerstein, R.G. Pembleton, R.C. Wilson, L.M. Ryan, High-resolution Nmr in randomly oriented solids with homonuclear dipolar broadening - combined multiple pulse nmr and magic angle spinning, J. Chem. Phys. 66 (1977) 361–362.
[12] L.M. Ryan, R.E. Taylor, A.J. Paff, B.C. Gerstein, Experimental-study of resolution of proton chemical-shifts in solids - combined multiple pulse Nmr and magic-angle spinning, J. Chem. Phys. 72 (1980) 508–515.
[13] K.R. Mote, V. Agarwal, P.K. Madhu, Five decades of homonuclear dipolar decoupling in solid-state NMR: Status and outlook, Prog. Nucl. Mag. Res. Sp. 97 (2016) 1–39.

[14] J.R. Lewandowski, J.N. Dumez, U. Akbey, S. Lange, L. Emsley, H. Oschkinat, Enhanced resolution and coherence lifetimes in the solid-state NMR spectroscopy of perdeuterated proteins under ultrafast magic-angle spinning, J. Phys. Chem. Lett. 2 (2011) 2205–2211.
[15] M. Hologne, V. Chevelkov, B. Reif, Deuterated peptides and proteins in MAS solid-state NMR, Prog. Nucl. Mag. Res. Sp. 48 (2006) 211–232.
[16] M. Mehring, J.S. Waugh, Magic-angle Nmr experiments in solids, Phys. Rev. B 5 (1972) 3459–4000.
[17] M.H. Levitt, A.C. Kolbert, A. Bielecki, D.J. Ruben, High-resolution 1H NMR in solids with frequency-switched multiple-pulse sequences, Solid State Nucl. Magn. Reson. 2 (1993) 151–163.
[18] E. Vinogradov, P.K. Madhu, S. Vega, High-resolution proton solid-state NMR spectroscopy by phase-modulated Lee-Goldburg experiment, Chem. Phys. Lett. 314 (1999) 443–450.
[19] E. Vinogradov, P.K. Madhu, S. Vega, Phase modulated Lee-Goldburg magic angle spinning proton nuclear magnetic resonance experiments in the solid state: a bimodal Floquet theoretical treatment, J. Chem. Phys. 115 (2001) 8983–9000.
[20] D. Sakellariou, A. Lesage, P. Hodgkinson, L. Emsley, Homonuclear dipolar decoupling in solid-state NMR using continuous phase modulation, Chem. Phys. Lett. 319 (2000) 253–260.
[21] A. Lesage, D. Sakellariou, S. Hediger, B. Elena, P. Charmont, S. Steuernagel, L. Emsley, Experimental aspects of proton NMR spectroscopy in solids using phase-modulated homonuclear dipolar decoupling, J. Magn. Reson. 163 (2003) 105–113.
[22] J.P. Amoureux, B. Hu, J. Trebosc, Enhanced resolution in proton solid-state NMR with very-fast MAS experiments, J. Magn. Reson. 193 (2008) 305–307.
[23] J.P. Amoureux, B.W. Hu, J. Trebosc, Q. Wang, O. Lafon, F. Deng, Homonuclear dipolar decoupling schemes for fast MAS, Solid State Nucl. Mag. 35 (2009) 19–24.
[24] M.E. Halse, L. Emsley, Improved phase-modulated homonuclear dipolar decoupling for solid-state NMR spectroscopy from symmetry considerations, J. Phys. Chem. A 117 (2013) 5280–5290.
[25] E. Salager, J.N. Dumez, R.S. Stein, S. Steuernagel, A. Lesage, B. Elena-Herrmann, L. Emsley, Homonuclear dipolar decoupling with very large scaling factors for high-resolution ultrafast magic angle spinning H-1 solid-state NMR spectroscopy, Chem. Phys. Lett. 498 (2010) 214–220.
[26] A. Lesage, L. Duma, D. Sakellariou, L. Emsley, Improved resolution in proton NMR spectroscopy of powdered solids, J. Am. Chem. Soc. 123 (2001) 5747–5752.
[27] S.P. Brown, A. Lesage, B. Elena, L. Emsley, Probing proton-proton proximities in the solid state: high-resolution two-dimensional 1H–1H double-quantum CRAMPS NMR spectroscopy, J. Am. Chem. Soc. 126 (2004) 13230–13231.
[28] M. Leskes, P.K. Madhu, S. Vega, Supercycled homonuclear dipolar decoupling in solid-state NMR: toward cleaner 1H spectrum and higher spinning rates, J. Chem. Phys. 128 (2008) 052309.
[29] M. Leskes, S. Steuernagel, D. Schneider, P.K. Madhu, S. Vega, Homonuclear dipolar decoupling at magic-angle spinning frequencies up to 65 kHz in solid-state nuclear magnetic resonance, Chem. Phys. Lett. 466 (2008) 95–99.
[30] S. Paul, R.S. Thakur, P.K. Madhu, H-1 homonuclear dipolar decoupling at high magic-angle spinning frequencies with rotor-synchronised symmetry, Chem. Phys. Lett. 456 (2008) 253–256.
[31] E. Salager, R.S. Stein, S. Steuernagel, A. Lesage, B. Elena, L. Emsley, Enhanced sensitivity in high-resolution H-1 solid-state NMR spectroscopy with DUMBO dipolar decoupling under ultra-fast MAS, Chem. Phys. Lett. 469 (2009) 336–341.
[32] S. Paul, R.S. Thakur, M. Goswami, A.C. Sauerwein, S. Mamone, M. Concistre, H. Forster, M.H. Levitt, P.K. Madhu, Supercycled homonuclear dipolar decoupling sequences in solid-state NMR, J. Magn. Reson. 197 (2009) 14–19.
[33] Z.H. Gan, P.K. Madhu, J.P. Amoureux, J. Trebosc, O. Lafon, A tunable homonuclear dipolar decoupling scheme for high-resolution proton NMR of solids from slow to fast magic-angle spinning, Chem. Phys. Lett. 503 (2011) 167–170.
[34] M.E. Halse, L. Emsley, A common theory for phase-modulated homonuclear decoupling in solid-state NMR, PCCP 14 (2012) 9121–9130.
[35] B. Elena, G. de Paepe, L. Emsley, Direct spectral optimisation of proton-proton homonuclear dipolar decoupling in solid-state NMR, Chem. Phys. Lett. 398 (2004) 532–538.
[36] E. Vinogradov, P.K. Madhu, S. Vega, Proton spectroscopy in solid state nuclear magnetic resonance with windowed phase modulated Lee-Goldburg decoupling sequences, Chem. Phys. Lett. 354 (2002) 193–202.
[37] Y. Nishiyama, Fast magic-angle sample spinning solid-state NMR at 60–100 kHz for natural abundance samples, Solid State Nucl. Mag. 78 (2016) 24–36.
[38] A. Samoson, T. Tuherm, Z. Gan, High-field high-speed MAS resolution enhancement in 1H NMR spectroscopy of solids, Solid State Nucl. Magn. Reson. 20 (2001) 130–136.
[39] E.L. Hahn, Spin Echoes, Phys. Rev. 80 (1950) 580–594.
[40] G. De Paepe, N. Giraud, A. Lesage, P. Hodgkinson, A. Bockmann, L. Emsley, Transverse dephasing optimized solid-state NMR spectroscopy, J. Am. Chem. Soc. 125 (2003) 13938–13939.
[41] M.H. Levitt, D.P. Raleigh, F. Creuzet, R.G. Griffin, Theory and simulations of homonuclear spin pair systems in rotating solids, J. Chem. Phys. 92 (1990) 6347–6364.
[42] E. Brunner, D. Freude, B.C. Gerstein, H. Pfeifer, Residual linewidths of Nmr-spectra of spin-1/2 systems under magic-angle spinning, J. Magn. Reson. 90 (1990) 90–99.
[43] L.J. Edwards, D.V. Savostyanov, A.A. Nevzorov, M. Concistre, G. Pileio, I. Kuprov, Grid-free powder averages: on the applications of the Fokker-Planck equation to solid state NMR, J. Magn. Reson. 235 (2013) 121–129.
[44] V.E. Zorin, S.P. Brown, P. Hodgkinson, Origins of linewidth in H-1 magic-angle spinning NMR, J. Chem. Phys. 125 (2006).
[45] Origin, in, OriginLab, Northampton, MA.
[46] C.H. Gorbitz, Crystal and molecular-structures of the isomeric dipeptides alpha-L-aspartyl-L-alanine and beta-L-aspartyl-L-alanine, Acta Chem. Scand. B 41 (1987) 679–685.
[47] C.R. Groom, I.J. Bruno, M.P. Lightfoot, S.C. Ward, The Cambridge Structural Database.
[48] U. Sternberg, F.-T. Koch, P. Losso, COSMOS Pro, COSMOS-Software, Jena, Germany.
[49] P. Hodgkinson, D. Sakellariou, L. Emsley, Simulation of extended periodic systems of nuclear spins, Chem. Phys. Lett. 326 (2000) 515–522.
[50] P. Hodgkinson, L. Emsley, Numerical simulation of solid-state NMR experiments, Prog. Nucl. Mag. Res. Sp. 36 (2000) 201–239.
[51] A. Lesage, M. Bardet, L. Emsley, Through-bond carbon-carbon connectivities in disordered solids by NMR, J. Am. Chem. Soc. 121 (1999) 10987–10993.
[52] I. Jakovkin, M. Klipfel, C. Muhle-Goll, A.S. Ulrich, B. Luy, U. Sternberg, Rapid calculation of protein chemical shifts using bond polarization theory and its application to protein structure refinement, PCCP 14 (2012) 12263–12276.
[53] R. Witter, L. Seyfart, G. Greiner, S. Reissmann, J. Weston, E. Anders, U. Sternberg, Structure determination of a pseudotripeptide zinc complex with the COSMOS-NMR force field and DFT methods, J. Biomol. Nmr 24 (2002) 277–289.
[54] U. Sternberg, Theory of the influence of the 2nd coordination sphere on the chemical-shift, Mol. Phys. 63 (1988) 249–267.
[55] H.J. Hogben, M. Krzystyniak, G.T.P. Charnock, P.J. Hore, I. Kuprov, Spinach - A software library for simulation of spin dynamics in large spin systems, J. Magn. Reson. 208 (2011) 179–194.
[56] MATLAB, The MathWorks, Inc., Natick, Massachusetts, United States.
[57] I. Kuprov, Fokker-Planck formalism in magnetic resonance simulations, J. Magn. Reson. 270 (2016) 124–135.
[58] J.O. Brauckmann, J.W.G. Janssen, A.P.M. Kentgens, High resolution triple resonance micro magic angle spinning NMR spectroscopy of nanoliter sample volumes, PCCP 18 (2016) 4902–4910.